D3.1 – List of coating candidates for air and fuel sides of interconnector plates

Project information

Project title	Advanced Processes Enabling Low cost and High Performing Large Scale Solid Oxide Electrolyser Production
Project acronym	PilotSOEL
Start date	01-06-2023
Type of action	HORIZON-JU-RIA
GA number	101112026
Duration	36 months
Project website	www.pilotSOEL.dtu.dk

Deliverable information

Deliverable number	*D3.1*
Deliverable title	*List of coating candidates for air and fuel sides of interconnector plates*
WP number	*WP3*
WP title	*Advanced surface coating technologies for IC plate*
WP leader	*NACO*
Responsible partner	*ELCOY*
Contributing partners	*NACO*
Authors	*Jouni Puranen*
Contributors	*Janis Zideluns*
Deliverable type	*R*
Dissemination level	*PU*
Contractual deadline	*31-08-2023*
Delivery date to EC	*31-08-2023*

Co-funded by the European Union

Clean Hydrogen Partnership

The project is supported by the Clean Hydrogen Partnership and its members.

1. Abstract

Solid oxide electrolysers (SOEL) are critical for efficient hydrogen production but face challenges such as chromium (Cr)-poisoning and materials degradation, specifically in their interconnector components made of ferritic stainless steels (FSS). WP3 focuses on developing optimized coatings for both the air and fuel sides of these interconnectors to improve electrical performance and extend lifespan. This deliverable D3.1 focuses on listing potential coating candidates that have shown promising results, as reported in various scientific journals, for use on both on fuel and airside of the SOEL stack. On the air side, Cu-doped spinel coatings have emerged as promising candidates, offering excellent Cr-barrier properties and superior electrical conductivity, while also addressing ethical and sustainability concerns associated with cobalt usage. On the fuel side, a multi-layered approach involving ceria (CeO_2) as a diffusion barrier has been proposed to mitigate issues like nickel diffusion into FSS and to maintain electrical and mechanical compatibility. The coatings aim to balance high technical performance with material sustainability, offering a pathway for the development of more durable and efficient SOEL systems.

2. Introduction

Solid oxide electrolysers have gained significant attention for their role in efficient hydrogen production. These stacks consist of an array of components including ceramic cells, interconnectors, and gasket structures. Interconnectors are predominantly manufactured from high chromium content (18-22 wt% of Cr) ferritic stainless steels (FSS) like Crofer 22 APU/H, AISI 441, and AISI 444. While these materials exhibit excellent mechanical properties and capability to form protective Cr_2O_3 oxide layers on the air side, they also present challenges including the degradation of electrical performance.

WP3 aims to systematically evaluate potential coatings for the air and fuel sides of the interconnector plates in SOEL stacks to enhance their performance and extend their lifespan. WP3 address the critical problem of chromium (Cr)-rich oxide scales which, while protective, can have detrimental impacts on SOEL performance. These scales can lead to cell degradation via Cr-poisoning, increased ohmic resistance, and thereby reduced stack performance. On the fuel side, the coatings also need to inhibit the diffusion of nickel into ferritic stainless steels and improve electrical contact points between the interconnectors and the ceramic cells.

Various coating candidates will be assessed based on their ability to 1) inhibit the continuous growth of Cr-rich oxide scales, 2) prevent the transport of Cr-species to the cathode, and 3) enhance overall stack performance by improving electrical contacts and minimizing materials degradation. Deliverable 3.1 will provide a comprehensive list of suitable coating materials, along with their potential advantages, offering a roadmap for subsequent work packages.

3. Coatings on the air side

Building upon the challenges outlined, a focal point of concern in the use of high chromium content FSS as interconnector materials in SOEL stacks is the phenomenon of Cr-poisoning. At the typical operating temperatures of 600-800 °C, these steels naturally form a Cr_2O_3 layer, which serves as a protective barrier against corrosion and degradation. However, the presence of humidity in the air exacerbates oxidation rates. Specifically, Cr_2O_3 reacts with water molecules and oxygen to form various chromium oxides and oxyhydroxides such as CrO_3, $CrO_2(OH)_2$, and $CrO_2(OH)$, as outlined in reaction equations 1-3 [1, 2].

$$2Cr_2O_3(s) + 3O_2(g) \leftrightarrow 4CrO_3(g) \quad (1)$$

$$2Cr_2O_3(s) + 3O_2(g) + 4H_2O(g) \leftrightarrow 4CrO_2(OH)_2(g) \quad (2)$$

$$Cr_2O_3(s) + O_2(g) + H_2O(g) \leftrightarrow 2CrO_2(OH)(g). \quad (3)$$

Notably, the partial pressures of $CrO_3(g)$ in dry air and $CrO_2(OH)_2(g)$ in humid air are the highest over $Cr_2O_3(s)$, indicating their dominant role in the air side atmosphere [1-3]. These Cr species are transported to the triple-phase boundary (TPB). This is the shared interface of the electrolyte, the air electrode, and the gas phase. Subsequent electrochemical reduction cycles them back to Cr_2O_3. Over time, this continuous reduction reaction of Cr species leads to a blocking of effective TPB sites. The consequence is a decrease in the electrochemical performance of the cell, manifesting as degradation, commonly termed as Cr-poisoning.

Given this complexity, the coatings applied on the air side must not only suppress the formation of Cr-rich oxide scales but also mitigate the transport of these problematic Cr species to the active reaction sites. Therefore, selecting appropriate coating materials and deposition process through parameters optimization can effectively address this issue.

Optimizing coating together with deposition technique must fulfil several requirements which are crucial for stack performance. These criteria include:

- Low diffusion coefficient for Cr ions and minimal transport of Cr compounds to inhibit Cr-poisoning [4].
- Excellent electrical conductivity, aiming for 100 % electronic conduction to minimize ohmic losses [5].
- Chemical, microstructural, and phase stability at stack operating temperatures in oxidizing and reducing conditions [5].
- Coefficient of Thermal Expansion (CTE) compatibility with other stack components, such as metallic interconnectors and air electrodes [5].
- High-temperature strength, along with creep and spallation resistance, to ensure long-term durability [5].
- Cost-effectiveness in mass production to facilitate broader commercial adoption [5].

Current research has identified several promising material compositions, particularly from the perovskite $(A,B)_2O_3$ and spinel $(A,B)_3O_4$ groups. $(Mn,Co)_3O_4$-based spinels such as $MnCo_2O_4$, Mn_2CoO_4 and $Mn_{1.5}Co_{1.5}O_4$ have shown particular promise, demonstrating both cubic and tetragonal crystal structures.

These $(Mn,Co)_3O_4$ spinels exhibit a lower rate of Cr transport and show even better Cr-barrier properties compared to perovskites [6,7]. The average electrical conductivity for $(Mn,Co)_3O_4$ spinel is 20.6 S/cm, with the highest conductivity observed for $Mn_{1.5}Co_{1.5}O4$ at 26 S/cm (Table 1). Moreover, the compatibility of their CTE with FSS and perovskite-type air electrodes is an added advantage.

However, one critical factor that this project considers is the reduction in the use of critical raw materials (CRM), notably cobalt and manganese [8]. This is a concern as a significant portion of cobalt ore is sourced from regions with high supply chain risks, such as the Democratic Republic of Congo. Additionally, cobalt compounds have potentially carcinogenic properties, complicating human interactions during manufacturing. Given these considerations, the materials tested in PilotSOEL will balance between performance optimization and responsible materials usage. The aim is to explore alternatives that not only meet the stringent technical requirements but also are less reliant on CRMs, thereby ensuring a sustainable and ethically sound approach to improving SOEL stack performance and durability.

3.1 Cobalt-less coating options

WP3 also explores cobalt-less coating options for the interconnectors. According to numerous scientific studies, copper (Cu) emerges as a promising alternative to cobalt (Table 1). Experiments have been conducted in which Co was either partially or completely replaced with Cu in the formulation of spinel coatings. These studies indicate that Cu-doped spinel coatings offer comparable Cr-barrier properties to their Co-containing counterparts. For instance, one experiment showcased that no Cr migration was observed on the LSCF cathode after 1000 hours at 800 °C when Cu-doped spinel was applied [9]. Similarly, a longevity test conducted on SUS 430 ferritic stainless steel coated with $(Mn,Co,Cu)_3O_4$ at 750 °C for 2000 hours also showed no noticeable Cr migration [10], underlining the efficacy of copper as a cobalt replacement.

One advantage of Cu-doped spinel coatings is their superior electrical conductivity. Based on an analysis of 17 different scientific journals (Table 1), the average electrical conductivity for $(Mn,Cu)_3O_4$ spinels was found to be approximately 53 S/cm, a value that markedly outperforms the Co-based spinels. In some cases, the electrical conductivity was almost 120 S/cm. This enhancement in electrical conductivity not only fulfils the technical requirement of high electronic conduction but also implies potential benefits in reducing ohmic losses in the SOEL stack.

Table 1. Electrical conductivity values of Mn-Co-Cu-O spinels at 650 °C

σ (S/cm) at 650	Composition	Mn	Co	Cu	Ni	Cr	Ti	Fe	Ref.
119,9	$Cu_{1.3}Mn_{1.7}O_4$	1,7		1,3					[11]
94,8	$Cu_{0.77}Ni_{0.45}Mn_{1.78}O_4$	1,78		0,77	0,45				[12]
85,9	Mn_2CuO_4	2		1					[13]
79,4	$Mn_{1.33}Co_{1.17}Cu_{0.5}O_4$	1,33	1,17	0,5					[14]
70,4	$Cu_{1.1}Mn_{1.9}O_4$	1,9		1,1					[11]
69,2	$Mn_{1.8}Cu_{1.2}O_4$	1,8		1,2					[13]
68,8	$Mn_{1.57}Co_{0.93}Cu_{0.5}O_4$	1,57	0,93	0,5					[14]
67,2	$MnCu_{0.5}Co_{1.5}O_4$	1	1,5	0,5					[15]

66,4	$MnCu_{0.5}Co_{1.4}O_4$	1	1,4	0,5					[10]
58,3	$CuMn_2O_4$	2		1					[16]
56,6	$Co_{0.9}Cu_{0.6}Mn_{1.5}O_4$	1,5	0,9	0,6					[16]
55,8	$MnCu_{0.7}Co_{1.3}O_4$	1	1,3	0,7					[10]
54,3	$Cu_{1.38}Mn_{1.62}O_4$	1,62		1,38					[17]
54,1	$Mn_{1.6}Cu_{1.4}O_4$	1,6		1,4					[13]
51,7	$Cu_{1.19}Mn_{1.81}O_4$	1,81		1,19					[17]
49,1	$Co_{1.2}Cu_{0.3}Mn_{1.5}O_4$	1,5	1,2	0,3					[16]
48,5	$Cu_{1.4}Mn_{1.6}O_4$	1,6		1,4					[18]
47,6	$CuMn_2O_4$	2		1					[11]
47,3	$Cu_{1.28}Mn_{1.72}O_4$	1,72		1,28					[17]
45,2	$Co_{0.5}CuMn_{1.5}O_4$	1,5	0,5	1					[16]
45,1	$Mn_{1.5}Co_{1.5}O_4$	1,5	1,5						[19]
44,7	$Co_{1.37}Cu_{0.63}MnO_4$	1	1,37	0,63					[16]
41,7	$Mn_{1.5}Cu_{1.5}O_4$	1,5		1,5					[13]
41,6	$Co_{1.7}Cu_{0.3}MnO_4$	1	1,7	0,3					[16]
39,2	$Cu_{0.3}Mn_{1.1}Co_{1.6}O_4$	1,1	1,6	0,3					[20]
38,5	$Cu_{1.58}Mn_{1.42}O_4$	1,42		1,58					[17]
38,3	$Mn_{1.4}Co_{1.4}Cu_{0.2}O_4$	1,4	1,4	0,2					[21]
37,6	$Cu_{0.9}Mn_{2.1}O_4$	2,1		0,9					[11]
37,0	$Cu_{1.47}Mn_{1.53}O_4$	1,53		1,47					[17]
36,0	$MnCo_2O_4$	1	2						[14]
33,9	$Mn_{1.25}Co_{1.75}O_4$	1,25	1,75						[14]
33,7	$Cu_{1.18}Mn_{1.82}O_4$	1,82		1,18					[12]
33,5	$Mn_{1.5}Co_{1.5}O_4$	1,5	1,5						[22]
32,5	$Co_{0.67}Cu_{0.33}Mn_2O_4$	2	0,67	0,33					[16]
31,1	$MnCu_{0.3}Co_{1.7}O_4$	1	1,7	0,3					[10]
29,3	$Mn_{1.5}Co_{1.5}O_4$	1,5	1,5						[23]
28,2	Co_2MnO_4	1	2						[16]
27,2	$Mn_{1.4}Co_{1.4}Cu_{0.2}O_4$	1,4	1,4	0,2					[9]
25,8	$MnCu_{0.1}Co_{1.9}O_4$	1	1,9	0,1					[10]
25,1	$Mn_{2.05}Co_{0.45}Cu_{0.5}O_4$	2,05	0,45	0,5					[14]
24,4	$Cu_{0.1}Mn_{1.2}Co_{1.7}O_4$	1,2	1,7	0,1					[20]
24,4	$Cu_{0.5}MnCo_{1.5}O_4$	1	1,5	0,5					[20]
24,0	$Mn_{1.5}Co_{1.5}O_4$	1,5	1,5						[14]
23,5	$Co_{0.5}Cu_{0.5}Mn_2O_4$	2	0,5	0,5					[16]
22,2	$CuCo_2O_4$		2	1					[24]
19,3	$Mn_{1.25}Co_{1.75}O_4$	1,25	1,75						[20]

18,8	$Mn_{1.4}Co_{1.4}Ni_{0.2}O_4$	1,4	1,4		0,2				[9]
18,8	$Mn_{1.5}Co_{1.5}O_4$	1,5	1,5						[9]
17,8	$Mn_{1.5}Co_{1.5}O_4$	1,5	1,5						[13]
17,7	$MnCo_2O_4$	1	2						[19]
16,9	$MnCo_2O_4$	1	2						[19]
16,5	$Mn_{1.5}Co_{1.5}O_4$	1,5	1,5						[16]
14,8	$Co_{0.67}Cu_{0.33}Mn_2O_4$	2	0,67	0,33					[16]
12,8	$MnCo_{1.66}Ti_{0.34}O_4$	1	1,66				0,34		[19]
11,7	$MnCo_2O_4$	1	2						[25]
11,7	$MnCo_{1.9}Fe_{0.1}O_4$	1	1,9					0,1	[25]
11,5	$MnCo_2O_4$	1	2						[26]
11,2	$MnCo_{1.75}Fe_{0.25}O_4$	1	1,75					0,25	[25]
10,3	$Mn_{1.25}Co_{1.25}Cr_{0.5}O_4$	1,25	1,25			0,5			[22]
9,7	$MnCo_2O_4$	1	2						[23]
9,0	$MnCo_2O_4$	1	2						[19]
8,8	$Cu_{1.08}Mn_{1.92}O_4$	1,92		1,08					[17]
7,4	$Co_{0.8}Cu_{0.2}Mn_2O_4$	2	0,8	0,2					[16]
5,0	$MnCo_{1.5}Fe_{0.5}O_4$	1	1,5					0,5	[25]
4,0	$NiMn_2O_4$	2			1				[23]
2,9	$MnCoCrO_4$	1	1			1			[26]
2,7	$MnCoFeO_4$	1	1					1	[25]
1,8	$CoMn_2O_4$	2	1						[16]
1,0	$MnCoCrO_4$	1	1			1			[19]
0,9	$MnCoCrO_4$	1	1			1			[22]
0,4	$CuFe_2O_4$			1				2	[27]
0,2	$CoFe_2O_4$		1					2	[28]
0,2	$Mn_{0.75}Co_{0.75}Cr_{1.5}O_4$	0,75	0,75			1,5			[22]
0,1	$MnCr_2O_4$	1				2			[23]
0,1	$MnCo_{1.66}Ti_{0.34}O_4$	1	1,66				0,34		[29]
0,1	$MnCo_{1.66}Fe_{0.34}O_4$	1	1,66					0,34	[29]
0,1	$Mn_{0.4}Co_{0.6}Cr_2O_4$	0,4	0,6			2			[19]
0,1	$Mn_{0.5}Co_{0.5}Cr_2O_4$	0,5	0,5			2			[22]
0,1	$MnCr_2O_4$	1				2			[26]

Building on the promising results of cobalt-less coating options, the list of candidate materials will feature copper-based alternatives that align with both stringent performance criteria and ethical considerations concerning the use of CRMs. Particularly noteworthy among these candidates is the composition Mn_2CuO_4, which has shown remarkable promise in preliminary studies. Further analysis conducted

through regression techniques, reveals that the $Mn_{1,5}Co_{0,75}Cu_{0,75}O_4$ composition achieved the improved electrical conductivity, reaching as high as 110 S/cm at an operating temperature of 650°C. This compelling finding reinforces copper's potential as an effective and sustainable substitute for cobalt in SOEL interconnector coatings.

In the PilotSOEL, the protective coatings are being manufactured using the PVD process. This process has the advantage of producing thinner and denser coatings compared to today's state-of-the-art processes. Theoretically, the conductivity should be greater than 30 S/cm with the coating thickness of 1.5 µm, typically produced with the PVD process, in order to achieve an ASR value less than 5 $m\Omega.cm^2$. The clear advantage here is that coatings with a dense microstructure can be produced, thereby minimizing the oxidation of the interconnect and the growth of less electrically conductive Cr-scale.

4. Coatings on the fuel side

While a great deal of research has focused on air-side coatings to mitigate issues of Cr-poisoning in FSS interconnectors, there has been comparatively less attention on fuel-side coatings. This area is equally critical, especially when ceramic cells are integrated with a nickel-contact layer. The contact layer, which could either be a separate mesh or a screen-printed layer, is typically applied on top of a nickel/yttria-stabilized zirconia (Ni/YSZ) supporting anode layer. Several challenges arise due to interactions at elevated temperatures between the various elements in the stack.

Firstly, nickel (Ni) has a tendency to diffuse into FSS at high operating temperatures (Figure 1). This diffusion alters the FSS to an austenitic grade, which has significantly different mechanical properties compared to FSS. One key difference is in the coefficient of thermal expansion (CTE), which becomes 18×10^{-6} K^{-1} for the altered material, in contrast to the $10\text{-}11\times10^{-6}$ K^{-1} exhibited by other stack components. This mismatch in CTE can result in mechanical stress and structural instability, potentially compromising the integrity of the SOEL stack [30, 31].

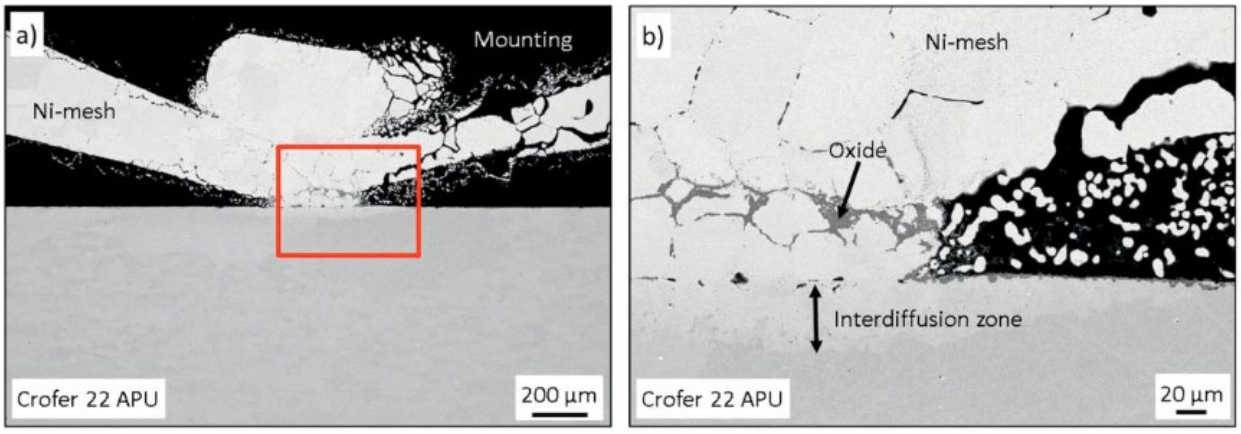

Figure 1. Interdiffusion zone of Ni and FSS interconnect [30]

Secondly, there is the issue of chromium (Cr) and iron (Fe) diffusing into the nickel layer. When this occurs, oxides form that have lower electrical conductivity compared to pure nickel. This can negatively impact the stack's overall performance by increasing ohmic resistance and thereby decreasing efficiency [31].

Given these considerations, coatings for the fuel side must be designed to prevent interdiffusion of nickel, chromium, and iron, while maintaining electrical and mechanical compatibility with the entire SOEL stack. Such fuel-side coatings would ideally also meet the same criteria for chemical, microstructural, and phase stability, high-temperature strength, and cost-effectiveness that are required for air-side coatings.

4.1 Diffusion barrier

To mitigate material diffusion and other challenges on the fuel side, various oxide-based coatings have been investigated. The fundamental requirement for these coatings is to exhibit excellent electronic conductivity under low oxygen partial pressures. One such material that has drawn interest is strontium titanates; however, their performance is highly sensitive to doping concentrations, which can limit their utility [31].

A thermodynamically stable alternative is ceria (CeO_2), which demonstrates acceptable electrical conductivity across a wide range of oxygen partial pressures. With an electrical conductivity value of 0.3 S/cm, CeO_2 performs notably better than either Cr_2O_3 (0.01 S/cm) or $MnCr_2O_4$ (0.001 S/cm) layers. These latter compounds can naturally form on the surface of unprotected FSS even on the fuel side, thereby compromising stack performance [31].

Because CeO_2 offers superior electrical conductivity compared to, for example, Mn-Cr-O spinels, it is advantageous for use as a diffusion barrier, particularly when transitioning to more affordable steel grades such as AISI 441 and 444. These grades are known to form thicker oxide scales on both the air and fuel sides, making a high-conductivity barrier like CeO_2 more critical for maintaining stack performance.

To further optimize the system, multi-layered structures can be employed on the fuel side. For instance, integrating a conductive Cu layer between the FSS and the CeO_2 layer can decrease the area-specific resistance (ASR) values compared to using a single layer of CeO_2 on top the FSS. [31] A similar strategy can be applied to the other side of the coating. By adding a conductive Ni layer on top of the CeO_2, one can potentially enhance the area of electrical contact between the cell and the FSS interconnect, thereby improving the overall electrical performance of the SOEL stack.

These multi-layered approaches offer a flexible, high-performance solution that addresses the complex requirements for fuel-side coatings, providing an additional layer of optimization in the pursuit of efficient and durable SOEL stacks.

5. Conclusion

The challenges associated with SOEL stacks, ranging from Cr-poisoning to the diffusion of elements like nickel, chromium, and iron, emphasise the need for innovative coating solutions for both the air and fuel sides of the interconnector plates. On the air side, Cu-doped spinel coatings, particularly Mn_2CuO_4, have

emerged as promising candidates that satisfy performance, ethical, and sustainability criteria. They offer excellent Cr-barrier properties and enhanced electrical conductivity.

On the fuel side, multi-layered structures involving ceria as a diffusion barrier, coupled with conductive layers of Cu and Ni, hold the potential to mitigate material diffusion issues and improve overall stack performance. These coating compositions, which balance technical performance with material sustainability from the CRM point of view, present a promising route for the future development of more efficient and durable SOEL stacks.

Coatings to be tested: $Mn_{1.5}Co_{1.5}O_4$ (air side coating, reference)

Mn_2CuO_4 (air side coating)

$Mn_{1,5}Co_{0,75}Cu_{0,75}O_4$ (air side coating)

CeO_2 (fuel side coating)

Cu-CeO_2 (fuel side coating)

Cu-CeO_2-Ni (fuel side coating)

6. List of references

[1] C. Gindorf, L. Singheiser, and K. Hilpert, "Vaporisation of chromia in humid air," *Journal of Physics and Chemistry of Solids*, vol. 66, no. 2–4, pp. 384–387, Apr. 2005, doi: 10.1016/j.jpcs.2004.06.092.

[2] K. Hilpert, D. Dos, M. Miller, D. H. Peck, and R. Weiss, "Chromium Vapor Species over Solid Oxide Fuel Cell Interconnect Materials and Their Potential for Degradation Processes," *J Electrochem Soc*, vol. 143, no. 11, pp. 3642–3647, 1996.

[3] J. FERGUS, "Effect of cathode and electrolyte transport properties on chromium poisoning in solid oxide fuel cells," *Int J Hydrogen Energy*, vol. 32, no. 16, pp. 3664–3671, Nov. 2007, doi: 10.1016/j.ijhydene.2006.08.005.

[4] W. Z. Zhu and S. C. Deevi, "Opportunity of metallic interconnects for solid oxide fuel cells: a status on contact resistance," *Mater Res Bull*, vol. 38, no. 6, pp. 957–972, May 2003, doi: 10.1016/S0025-5408(03)00076-X.

[5] W. Z. Zhu and S. C. Deevi, "Development of interconnect materials for solid oxide fuel cells," *Materials Science and Engineering A*, vol. 348, no. 1–2, pp. 227–243, May 2003, doi: 10.1016/S0921-5093(02)00736-0.

[6] Y. Fang, C. Wu, X. Duan, S. Wang, and Y. Chen, "High-temperature oxidation process analysis of MnCo2O4 coating on Fe–21Cr alloy," *Int J Hydrogen Energy*, vol. 36, no. 9, pp. 2–7, Mar. 2011, doi: 10.1016/j.ijhydene.2011.01.130.

[7] N. J. Magdefrau, L. Chen, E. Y. Sun, J. Yamanis, and M. Aindow, "Formation of spinel reaction layers in manganese cobaltite-coated Crofer22 APU for solid oxide fuel cell interconnects," *J Power Sources*, vol. 227, pp. 318–326, Apr. 2013, doi: 10.1016/j.jpowsour.2012.07.091.

[8] European Commission, "Report on Critical Raw Materials for the EU," 2014.

[9] B. K. Park *et al.*, "Cu- and Ni-doped Mn1.5Co1.5O4 spinel coatings on metallic interconnects for solid oxide fuel cells," *Int J Hydrogen Energy*, vol. 38, no. 27, pp. 12043–12050, 2013, doi: 10.1016/j.ijhydene.2013.07.025.

[10] J. Xiao, W. Zhang, C. Xiong, B. Chi, J. Pu, and L. Jian, "Oxidation behavior of Cu-doped MnCo2O4 spinel coating on ferritic stainless steels for solid oxide fuel cell interconnects," *Int J Hydrogen Energy*, vol. 41, no. 22, pp. 9611–9618, 2016, doi: 10.1016/j.ijhydene.2016.03.051.

[11] N. Hosseini, F. Karimzadeh, M. H. Abbasi, and G. M. Choi, "Microstructural characterization and electrical conductivity of Cu xMn3-xO4 (0.9<x<1.3) spinels produced by optimized glycine-nitrate combustion and mechanical milling processes," *Ceram Int*, vol. 40, no. 8 PART A, pp. 12219–12226, 2014, doi: 10.1016/j.ceramint.2014.04.065.

[12] S. Joshi and A. Petric, "Nickel substituted CuMn2O4 spinel coatings for solid oxide fuel cell interconnects," *Int J Hydrogen Energy*, vol. 42, no. 8, pp. 6–11, 2016, doi: 10.1016/j.ijhydene.2016.08.075.

[13] N. S. Waluyo *et al.*, "(Mn,Cu)3O4-based conductive coatings as effective barriers to high-temperature oxidation of metallic interconnects for solid oxide fuel cells," *Journal of Solid State Electrochemistry*, vol. 18, no. 2, pp. 445–452, 2014, doi: 10.1007/s10008-013-2245-6.

[14] A. Masi *et al.*, "Cu-Mn-Co oxides as protective materials in SOFC technology: The effect of chemical composition on mechanochemical synthesis, sintering behaviour, thermal expansion and electrical conductivity," *J Eur Ceram Soc*, vol. 37, no. 2, pp. 661–669, 2017, doi: 10.1016/j.jeurceramsoc.2016.09.025.

[15] J. Xiao, W. Zhang, C. Xiong, B. Chi, J. Pu, and L. Jian, "Oxidation of MnCu0.5Co1.5O4 spinel coated SUS430 alloy interconnect in anode and cathode atmospheres for intermediate temperature solid oxide fuel cell," *Int J Hydrogen Energy*, vol. 40, no. 4, pp. 1868–1876, 2015, doi: 10.1016/j.ijhydene.2014.11.124.

[16] Y. Wang, "Structure and Electrical Conductivity of Mn-based Spinels Used as Solid Oxide Fuel Cell Interconnect Coatings," McMaster University, 2013.

[17] B. E. Martin and A. Petric, "Electrical properties of copper-manganese spinel solutions and their cation valence and cation distribution," *Journal of Physics and Chemistry of Solids*, vol. 68, no. 12, pp. 2262–2270, 2007, doi: 10.1016/j.jpcs.2007.06.019.

[18] S. Zhen *et al.*, "High performance cobalt-free Cu1.4Mn1.6O4 spinel oxide as an intermediate temperature solid oxide fuel cell cathode," *J Power Sources*, vol. 315, pp. 140–144, 2016, doi: 10.1016/j.jpowsour.2016.03.046.

[19] J. W. Fergus, K. Wang, and Y. Liu, "Transition Metal Spinel Oxide Coatings for Reducing Chromium Poisoning in SOFCs," vol. 33, no. 40, pp. 77–84, 2011, doi: 10.1149/1.3589187.

[20] T. Brylewski, A. Kruk, M. Bobruk, A. Adamczyk, J. Partyka, and P. Rutkowski, "Structure and electrical properties of Cu-doped Mn-Co-O spinel prepared via soft chemistry and its application in intermediate-temperature solid oxide fuel cell interconnects," *J Power Sources*, vol. 333, pp. 145–155, 2016, doi: 10.1016/j.jpowsour.2016.09.136.

[21] G. Chen *et al.*, "Mn1.4Co1.4Cu0.2O4 spinel protective coating on ferritic stainless steels for solid oxide fuel cell interconnect applications," *J Power Sources*, vol. 278, pp. 230–234, 2015, doi: 10.1016/j.jpowsour.2014.12.070.

[22] Y. Liu, J. W. Fergus, and C. Dela Cruz, "Electrical properties, cation distributions, and thermal expansion of manganese cobalt chromite spinel oxides," *Journal of the American Ceramic Society*, vol. 96, no. 6, pp. 1841–1846, 2013, doi: 10.1111/jace.12254.

[23] Z. YANG, G. XIA, X. LI, and J. STEVENSON, "(Mn,Co)3O4 spinel coatings on ferritic stainless steels for SOFC interconnect applications," *Int J Hydrogen Energy*, vol. 32, no. 16, pp. 3648–3654, Nov. 2007, doi: 10.1016/j.ijhydene.2006.08.048.

[24] P. Paknahad, M. Askari, and M. Ghorbanzadeh, "Characterization of nanocrystalline CuCo2O4 spinel prepared by sol???gel technique applicable to the SOFC interconnect coating," *Appl Phys A Mater Sci Process*, pp. 727–734, 2015, doi: 10.1007/s00339-015-9021-7.

[25] T. Kiefer, M. Zahid, F. Tietz, D. Stöver, and Z. H.-R., "Electrical conductivity and thermal expansion coefficients of spinel in the series MnCo2-xFexO4 for application as a protective layer in SOFC," in *Proceeding of the 26th Riso International Symposium on Materials Science: Solid State Electrochmistry*, S. Linderoth, A. Smith, N. Bonanos, A. Hagen, L. Mikkelsen, K. Kammer, D. Lybye, P. V. Hendriksen, F. W. Poulsen, M. Mogensen, and W. G. Wang, Eds., Roskilde, 2005, pp. 261–266.

[26] X. Chen, P. Hou, C. Jacobson, S. Visco, and L. Dejonghe, "Protective coating on stainless steel interconnect for SOFCs: oxidation kinetics and electrical properties," *Solid State Ion*, vol. 176, no. 5–6, pp. 425–433, Feb. 2005, doi: 10.1016/j.ssi.2004.10.004.

[27] S. N. Hosseini, M. H. Enayati, F. Karimzadeh, N. M. Sammes, and A. M. Preparation, "Synthesizing CuFe2O4 Spinel Powders by a Combustion-Like Process for Solid Oxide Fuel Cell Interconnect Coatings," *International Journal of Chemical, Molecular, Nuclear, Materials and Metallurgical Engineering*, vol. 9, no. 7, pp. 857–860, 2015.

[28] Z. H. Bi, J. H. Zhu, and J. L. Batey, "CoFe2O4 spinel protection coating thermally converted from the electroplated Co–Fe alloy for solid oxide fuel cell interconnect application," *J Power Sources*, vol. 195, no. 11, pp. 3605–3611, Jun. 2010, doi: 10.1016/j.jpowsour.2009.12.011.

[29] K. Wang, Y. Liu, and J. W. Fergus, "Interactions Between SOFC Interconnect Coating Materials and Chromia," *Journal of the American Ceramic Society*, vol. 94, no. 12, pp. 4490–4495, Dec. 2011, doi: 10.1111/j.1551-2916.2011.04749.x.

[30] L. Niewolak, L. Blum, R. Peters, D. Grüner, and W. J. Quadakkers, "Behavior of Metallic Components During 4,000 h Operation of an SOFC Stack with Carbon Containing Fuel Gas," *Fuel Cells*, vol. 16, no. 5, pp. 600–610, Oct. 2016, doi: 10.1002/fuce.201600085.

[31] J. Froitzheim, L. Niewolak, M. Brandner, L. Singheiser, and W. J. Quadakkers, "Anode side diffusion barrier coating for solid oxide fuel cells interconnects," *J Fuel Cell Sci Technol*, vol. 7, no. 3, pp. 0310201–0310207, Jun. 2010, doi: 10.1115/1.3182731.